Spectrochimica Acta Part A: Molecular and Biomolecular Spectroscopy 253 (2021) 119579

Contents lists available at ScienceDirect

Spectrochimica Acta Part A: Molecular and Biomolecular Spectroscopy

journal homepage: www.elsevier.com/locate/saa

The relationship between solvatochromic properties and *in silico* ADME parameters of new chloroethylnitrosourea derivatives with potential anticancer activity and their β-Cyclodextrin complexes

Hassina Fisli [a,*], Andreas Hennig [b], Mohamed Lyamine Chelaghmia [c], Mohamed Abdaoui [a]

[a] Laboratory of Applied Chemistry, Université 8 Mai 1945 Guelma, Algeria
[b] Institute of Chemistry of New Materials, Universität Osnabrück, Germany
[c] Laboratory of Industrial Analysis and Materials Engineering, Université 8 Mai 1945 Guelma, Algeria

HIGHLIGHTS

- A new series of *N*-(2-chloroethyl)-*N*-nitrosourea (CENU) derivatives was synthesized.
- In silico ADME/Tox prediction study suggested CENUs as potential anticancer drugs.
- Solvatochromism of CENUs evaluated by the Kamlet-Taft, Catalán and Laurence models.
- Solvatochromic comparison method revealed excellent correlations.
- Host-guest complexes of the CENUs with β-CD were explored.

GRAPHICAL ABSTRACT

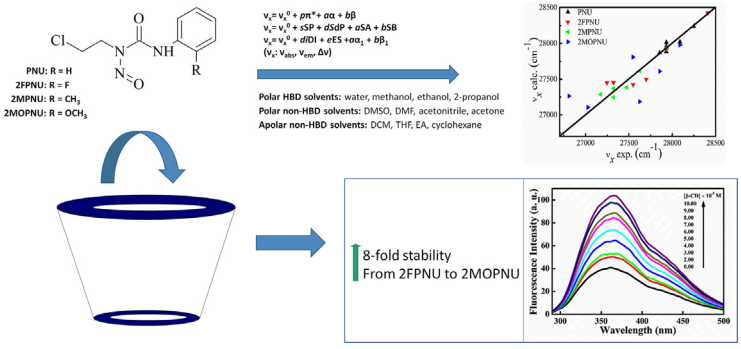

ARTICLE INFO

Article history:
Received 9 September 2020
Received in revised form 28 January 2021
Accepted 30 January 2021
Available online 13 February 2021

Keywords:
Nitrosourea
ADME/Tox
Solvatochromism
LSER
Spectrofluorimetry
β-cyclodextrin

ABSTRACT

In view of the anticancer effect of nitrosoureas a set of four new *N*-(2-chloroethyl)-*N*-nitrosourea (CENU) derivatives was synthesized. An *in silico* absorption, distribution, metabolism, excretion and toxicity (ADME/Tox) prediction study revealed that the CENU derivatives satisfied all the required criteria for oral administration and introduced them as remarkable anticancer candidates in the central nervous system (CNS). A comparative solvatochromic study including the Kamlet-Taft, Catalán and Laurence models indicated that the solvatochromic behavior of the CENUs depended on both, unspecific and specific solvent–solute interactions. In detail, the solvatochromic effect of the solvent polarity on the absorption and emission maxima was significant for all CENUs, whereas the solvatochromic effect of the solvent's ability to donate or accept hydrogen bonds on the absorption and emission maxima was critically dependent on the electron density of the *N*'-aryl group. From the solvatochromic comparison method, excellent correlations ($r \geq 0.890$) were obtained between the ADME parameters and the solvatochromic regression coefficients obtained by the Catalán model. As potential stabilizers, inclusion complexes of the investigated CENU derivatives with *β*-cyclodextrin (*β*-CD) were also explored. The spectrofluorimetric host–guest experiments included double-reciprocal Benesi-Hildebrand plots as well as the molar ratio and continuous variation plots (Job's plots), which established a 1:1 *β*-CD to CENU binding stoichiometry and relatively high affinities of *β*-CD for CENU derivatives.

* Corresponding author at: Laboratory of Applied Chemistry, Université 8 Mai 1945 Guelma, P.O. Box 401, 24000 Guelma, Algeria.
E-mail address: fisli.hassina@univ-guelma.dz (H. Fisli).

https://doi.org/10.1016/j.saa.2021.119579
1386-1425/

1. Introduction

Nitrosoureas and, in particular, *N*-(2-chloroethyl)-*N*-nitrosoureas (CENUs) are potential drug candidates for antitumor chemotherapy since they are active on a large number of tumors [1]. Given their potential, the chemistry of CENUs is very diverse and has been the object of intensive studies, which revealed that their primary mode of action involves alkylation, whereas other, yet to be confirmed mechanisms have been also invoked [1,2]. Previous structure–activity relationships found that small substituent changes can largely influence the chemical as well as the biological properties of CENUs, e.g., their cytotoxicity, mutagenicity, tumorigenicity, and control for histological variation of tumors [3]. For example, the alkylating activity of various *N*'-aryl-*N*-nitrosoureas in experimental medicinal studies has been related to the inductive effect and the hydrogen bond-forming ability of the substituents at the urea nitrogen atoms [4].

As a continuation of our previous work [5,6], we report herein a new series of CENUs derived from primary arylamines (aniline and anilines substituted at the ortho position: 2-fluoroaniline, 2-methylaniline and 2-methoxyaniline). The chemical structures of the synthesized CENU derivatives are summarized in Fig. 1 and include 1-(2-chloroethyl)-3-phenyl-1-nitrosourea (PNU), 1-(2-chloroethyl)-3-(2-fluorophenyl)-1-nitrosourea (2FPNU), 1-(2-chloroethyl)-3-(2-methylphenyl)-1-nitrosourea (2MPNU) and 1-(2-chloroethyl)-3-(2-methoxyphenyl)-1-nitrosourea (2MOPNU). The selection of CENUs examined in this study expands the common structural motifs that have been used in experimental medicinal studies [2,4,7] and introduces structural variations at the *ortho*-position of the *N*'-aryl group. This allows to dissect electronic factors from steric factors for controlling *in vitro* and *in vivo* actions of these compounds. The latter can be neglected in our series of CENUs [8], because the *ortho*-position of the *N*'-aryl group is thought to play no role as a reaction center in the generation of the active antitumor species [4].

The new CENU derivatives were successfully synthesized and characterized and their potential anticancer activity was assessed by *in silico* investigations of their absorption, distribution, metabolism, and excretion (ADME) properties. With the goal to study structure–activity relationships and to potentially relate the biological activity of CENUs to their physicochemical properties, a detailed solvatochromic study was performed to examine the effects of the various *ortho*-substituents on non-specific and specific interactions of the CENU derivatives with the surrounding solvent [9,10]. A better understanding of solvent–solute interactions has the potential to enhance the pharmacologically pertinent properties of CENUs and to improve their application potential as cancer chemotherapeutic agents. Therefore, the absorption and emission maxima and the Stokes shifts of the CENUs were evaluated with the Kamlet-Taft, Catalán, and Laurence et al. models for solvatochromic behavior in twelve different solvents and we found, in fact, significant correlations between the regression coefficients from the solvatochromic studies and the ADME parameters from the *in silico* studies of the CENU derivatives. In particular, excellent correlations ($r \geq 0.890$) were revealed between the solvatochromic analysis of selected solvent sets according to the Catalán model and the HIA, Caco-2, MDCK, BBB, and PPB ADME parameters.

Since the currently used CENUs are known to be quite unstable, too hydrophobic and of limited aqueous solubility, and often show major unfavorable side effects, the interaction of the new CENU derivatives with β-cyclodextrin (β-CD) was also investigated, which appears as an excellent candidate to optimize CENUs actions [2,11–13]. β-CD is widely used due to its low cost and its capacity to interact with a wide variety of molecules, including pesticides and drugs [5,6,14,15], and we determined herein the stoichiometry and binding constants (K) of the CENU/β-CD inclusion complexes by fluorescence spectroscopy [16–25]. The contribution of our research leads to provide a theoretical basis for developing new drugs, drug carriers, and new forms of drugs, and can be exploited in the future to obtain more detailed information about the CD inclusion process of CENUs.

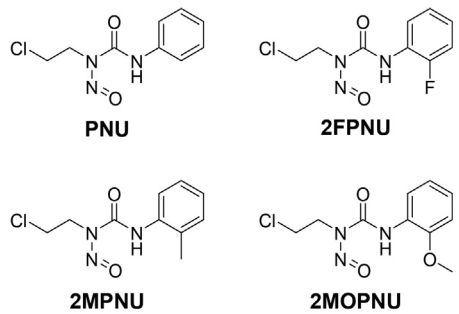

Fig. 1. Chemical structures of the CENU derivative molecules used in this study.

2. Experimental

2.1. Synthesis

The synthesis of CENU derivatives was performed according to a general procedure reported in Refs. [2,26] and the details of the synthesis are provided as Supplementary Material.

2.2. In silico ADME study

The ADMET parameters and the pharmacokinetic profile along with the druglikeness of the investigated CENU derivatives were evaluated by the freely offered web servers SwissADME-(http://www.swissadme.ch/) and PreADMET (https://preadmet.bmdrc.kr/).

2.3. Spectroscopic measurements

Fluorescence excitation (for ν_{abs}) and emission (for ν_{em}) spectra were recorded in 1-cm quartz glass cuvettes at room temperature on a Shimadzu RF-5301PC type spectrofluophotometer equipped with a Xenon lamp as excitation source. All the solutions were freshly prepared and mixed well by an UP50H ultrasonic processor (Hielscher Ultrasonics GmbH, Germany). All measurements were made at least in duplicate.

2.3.1. Solvatochromic studies

Stock solutions of the CENU derivatives were freshly prepared for each measurement in the respective solvent (methanol, ethanol, 2-propanol, dimethyl sulfoxide (DMSO), acetonitrile, dimethylformamide (DMF), acetone, dichloromethane (DCM), tetrahydrofuran (THF), ethyl acetate (EA) and cyclohexane) to obtain working solutions of 1.00×10^{-5} M. For measurements in water, CENU stock solutions in acetonitrile were diluted with water to afford solutions containing 2 vol% acetonitrile in water. Then, fluorescence excitation and emission spectra of the working solutions were recorded and the wavelengths of the excitation and emission maxima were converted into wavenumbers. Plots of the linear solvation energy relationship (LSER) were obtained by multiple linear regression analysis using Excel Solver. Therefore, the experimental absorption and emission maxima, ν_{abs} and ν_{em}, as well as the Stokes shift, $\Delta\nu = \nu_{abs} - \nu_{em}$, were used as the

solvent-dependent property in the Kamlet-Taft (v_x in Eq. 1), Catalán (A in Eq. 2), and Laurence (v_a in Eq. 3) models, which gave with the empirical solvatochromic model parameters (Table S1) the fitted lines including the respective regression and correlation coefficients.

2.3.2. Correlation analysis between solvatochromic behavior and ADME parameters

In order to reveal correlations of the solvatochromic regression coefficients and the ADME parameter, the respective values were plotted against each other and analyzed by linear regression analysis using Microsoft Office Excel Solver to obtain the correlation coefficients.

2.3.3. Host-guest studies with β-CD

Host-guest experiments of the CENUs with β-CD were performed at room temperature in acetonitrile. For the investigation of the effect of β-CD on the fluorescence properties of CENUs and for the determination of the binding constants, the concentration of each CENU derivative was kept constant at 1.00×10^{-5} M, while the β-CD concentration was varied from 0.00 to 10.00×10^{-5} M. Fluorescence data for the continuous variation plots (Job's plots) and molar ratio plots were obtained at 1.00×10^{-5} M total concentration of β-CD and CENU. All fluorescence spectra were measured using identical experimental conditions (excitation wavelength, monochromator slit widths, etc.).

3. Results and discussion

3.1. Synthesis of CENU derivatives

First, various arylamines (aniline, 2-fluoroaniline, 2-methylaniline and 2-methoxyaniline) were reacted with 2-chloroethyl isocyanate to afford the respective 2-chloroethylurea (CEU) derivatives (Fig. S1). The structure of the CEUs was confirmed by ^{1}H NMR spectroscopy, which indicated the presence of aromatic protons in the region from 6.95 to 9.50 ppm, by triplets attributed to the chloromethylene group in the range of 3.68 to 3.95 ppm and a quadruplet of the CH_2N group between 3.40 and 3.78 ppm, and by electrospray ionization mass spectrometry (ESI-MS), which gave the expected molecular ion peaks.

The subsequent nitrosation reaction was carried out with sodium nitrite, which is not regiospecific and gives the *N*'-aryl-*N*-nitrosoureas as major and the *N*'-aryl-*N*'-nitrosoureas as a minor product (Fig. S2) as revealed by thin layer chromatography. Separation of the two isomers by column chromatography on silica gel was, however, straightforward and the structure of the CENUs was confirmed by ^{1}H NMR spectroscopy and ESI-MS. In ESI-MS, all CENUs gave $[M-NO + H]^+$ ion peaks corresponding to the loss of NO due to the instability of the *N*-nitroso group under ESI-MS conditions [27].

In ^{1}H NMR, successful nitrosation was confirmed by disappearance of the exchangeable N-H protons and by appearance of an A_2X_2 system with a triplet between 3.10 and 3.75 ppm corresponding to the chloromethylene group and a triplet between 3.65 and 4.32 ppm corresponding to the CH_2NNO group. As expected, the nitroso group has a strong deshielding effect and the peak corresponding to the CH_2N group was significantly shifted downfield upon nitrosation. A challenge in the synthesis of CENUs is the regioselectivity of the nitrosation reaction [26,28], which may lead to the formation of two regioisomers (Fig. S3), from which only the *N*-(2-chloroethyl)-*N*-nitrosourea derivatives are of therapeutic interest, whereas the *N*-(2-chloroethyl)-*N*'-nitrosoureas cannot form a vinyl carbonium ion and, thus, lack oncostatic properties [1,2]. Under kinetic control, we were able to obtain the desirable *N*-(2-chloroethyl)-*N*-nitrosourea derivatives as the major product. In the cases of PNU, 2MPNU and 2MOPNU, double nitrosation has not been observed, which can be ascribed to steric constraints for 2MPNU and 2MOPNU as well as to an intramolecular hydrogen bond (Fig. S3) between the oxygen atom of the nitroso group and the hydrogen atom of the neighboring amide group [29].

3.2. In silico ADME predictions

Nowadays, modern drug discovery involves searching drug candidates with suitable absorption, distribution, metabolism, and excretion (ADME) properties to improve pharmacological activity. Therefore, *in silico* ADME screens became increasingly important to select the most promising compounds, because they minimize the risk of drug candidates failing in late-stage development and allow to reject compounds with inappropriate ADME properties before substantial time and money are invested in synthesis and testing [30]. The physicochemical properties and pharmacokinetic parameters of our synthesized CENU derivatives were determined *in silico* by the SwissADME and Pre-ADMET softwares to explore their drug-like characteristics and the principal descriptors are given in Tables 1 and 2.

With respects to the physicochemical properties displayed in Table 1, the investigated derivatives present zero violation for Lipinski's Rule of Five for oral drug availability: (1) The molecular weight (MW) of the CENU derivatives is between 227.65 and 257.67 g/mol and, thus, below 500 g/mol, which ensures easy transportation, absorption and diffusion of compounds; (2) the estimated octanol/water partition coefficients (log *P* values) were between 1.91 and 2.27 and, thus, lower than 4.15 suggesting a good permeability across the cell membrane; (3) the number of hydrogen bonds to be donated by the solute to the water molecules in an aqueous solution (HBD) is less than 5, one HBD for all the CENU derivatives; and (4) the number of hydrogen bonds to be accepted by the solute from the water molecules (HBA) is less than 10, between 3 and 4 HBA. Moreover, the number of rotatable bonds in the investigated derivatives were between 6 and 7 and, thus, less than 10, and the topological polar surface area (TPSA) was lower than 140 Å^2, namely 61.77 and 71.00 Å^2, with consequent percentages oral absorption (%ABS) of 87.68 and 84.50% suggesting good permeability, absorption and transport via biological membranes. Consequently, the examined CENU derivatives should theoretically manifest good oral availabilities as drugs. This was confirmed by high bioavailability scores of 0.55 for all the examined CENU derivatives and pan assay interference compounds (PAINS) presented zero alerts to all the hits. Finally, in accordance with our straight-forward synthesis, the synthetic accessibility scores of all the derivatives were between 2.22 and 2.41.

Additionally, *in silico* studies were performed using the Pre-ADMET software to obtain important pharmacokinetic parameters, namely Caco-2 (human colon adenocarcinoma) and MDCK (Madin-Darby canine kidney cells) permeability coefficients, the *in vitro* skin permeability, the percentage of human intestinal absorption (HIA), blood brain barrier partition coefficients (BBB), and percentage of human plasma protein binding (PPB). This allows a first assessment of the epithelial and endothelial permeability for oral and transdermal drug delivery. Moreover, the Pre-ADMET calculations include the Ames test for checking toxicity and a prediction for rodent carcinogenicity assay results. The results generated at this regard are shown in Table 2.

The efficacy of drugs, including anticancer drugs, is mainly dependent on the ability of the compounds to permeate across cell membranes [31]. When evaluating the absorption properties for the investigated CENU derivatives, HIA values showed that all the derivatives can be classified as well-absorbing compounds (70 to 100%) with high HIA values from 95.04 to 95.61%. They exhibited

Table 1
Swiss ADME physicochemical and ADME prediction of analyzed CENU derivatives.

Compd	Lipinski's parameters					nROTB[e]	TPSA[f]	%ABS[g]	BIO Score[h]	PAINS #alerts[i]	SAccess[j]
	MW[a]	Log *P*[b]	HBA[c]	HBD[d]	Violations						
PNU	227.65	1.91	3	1	0	6	61.77	87.68	0.55	0	2.22
2FPNU	245.64	2.27	4	1	0	6	61.77	87.68	0.55	0	2.41
2MPNU	241.67	2.25	3	1	0	6	61.77	87.68	0.55	0	2.27
2MOPNU	257.67	1.97	4	1	0	7	71.00	84.50	0.55	0	2.39

[a] Molecular weight (g/mol).
[b] Logarithm of partition coefficient between n-octanol and water.
[c] Number of H-bond acceptors (O and N atoms).
[d] Number H-bond donors (OH and NH groups).
[e] Number of rotatable bonds.
[f] Topological polar surface area (Å^2).
[g] Percentage of absorption.
[h] Bioavailability Score.
[i] Number of Pan Assay Interference Structures alerts.
[j] Synthetic Accessibility.

Table 2
pre-ADMET absorption, distribution, metabolism, excretion and toxicity prediction of analyzed CENU derivatives.

Compd	HIA (%)[a]	Caco-2 (nm/s)[b]	MDCK (nm/s) [c]	Skin_Permeability	BBB[d]	PPB (%)[e]	Ames_test	Carcino_Mouse	Carcino_Rat
PNU	95.14	15.20	39.61	−2.60	0.70	82.92	mutagen	negative	negative
2FPNU	95.61	20.37	129.45	−3.26	0.73	88.03	mutagen	positive	negative
2MPNU	95.37	10.93	56.19	−2.53	0.71	91.67	mutagen	positive	negative
2MOPNU	95.04	20.53	35.71	−3.26	0.83	74.59	mutagen	positive	negative

[a] Percentage of human intestinal absorption.
[b] Adenocarcenoma cell permeability.
[c] Maden Darby Canine Kidney cell permeability.
[d] Blood-Brain Barrier penetration.
[e] PlasmaProtein Binding.

medium cell permeability in Caco-2 (4 to 70 nm/s) and MDCK (25 to 500 nm/s) models with permeability coefficients ranging from 10.93 to 20.53 nm/s and 35.71 to 129.45 nm/s, respectively. In contrast, the skin permeability values were negative suggesting that transdermal delivery would not be a viable administration route for CENU derivatives.

Since *N*-nitrosourea-type anticancer drugs are especially applied in the central nervous system (CNS), their permeability through the BBB was the most interesting parameter. Generally, BBB values are a direct measure of penetration of a drug into the CNS. Compounds which exhibit BBB penetration values higher than 0.40 are considered as active in the CNS and compounds that have values below 0.40 are inactive in the CNS [32]. All the CENU derivatives analyzed showed penetration values higher than 0.40 ranging from 0.70 to 0.83. Thus, it is highly likely that they can cross the BBB and are active in the CNS. Moreover, the investigated derivatives showed PPB values lower than 90%, from 74.59 to 88.03, except 2MPNU (91.67%), which indicates that the compounds will not be trapped by too strong binding to proteins in the blood plasma.

The Ames test predicted that all the CENU derivatives are mutagens and the carcinogenicity prediction suggested that all the examined CENU derivatives except PNU are not carcinogenic in mice, but that they may be carcinogenic in rats.

In summary, the results of the evaluation of the ADME/Tox properties suggested that the investigated CENU derivatives satisfy all the required criteria for oral administration, which renders them suitable drug lead structures for further optimization and evaluation.

3.3. Solvatochromism of the CENU derivatives

The photophysical properties of molecules, such as the absorption and emission maxima, the shape of the spectral band, and the Stokes shift are influenced by the nature and the position of functional groups in the molecule, by the geometry of the molecule in the ground and excited states, and by the nature of the surrounding solvent environment [33]. Molecules with solvent-sensitive spectroscopic properties are very common, but it is often challenging to provide an unambiguous explanation of the origin of this solvent dependence. Therefore, considerable efforts have been deployed to correlate spectral properties with macroscopic and empirical solvent parameters [34].

The solvent effect has been estimated with Kamlet-Taft [35], Catalán [36] and Laurence et al. models [37]. The solvation effects treatment supposes attractive solute–solvent interactions and allows evaluating the ability of examined compounds to interact with the surrounding media. These methods treat specific and non-specific types of solute–solvent interactions separately, which gives their importance and significance. This knowledge can be used to extrapolate the dependence of these spectral properties in several solvents and to establish the nature of environments in macromolecules.

The photophysical properties of the CENU derivatives were investigated to determine the effect of substituent, to examine the solvatochromic properties, and to find out the effect of non-specific and specific interactions with the surrounding solvents for the investigated CENU derivatives. Therefore, absorption and emission spectra were measured in solvents of different types with varying polarity, polarizability, hydrogen bond donating (HBD) ability (protic solvents) and hydrogen bond accepting (HBA) ability (aprotic solvents), namely the polar HBD solvents water, methanol, ethanol, and 2-propanol, the polar non-HBD solvents dimethyl sulfoxide (DMSO), dimethyl formamide (DMF), acetonitrile, and acetone, and the apolar, non-HBD solvents DCM, THF, EA, and cyclohexane. The resulting absorption and emission frequencies and Stokes shifts of the CENU derivatives investigated in selected solvents are presented in Table 3.

Table 3
Absorption and emission frequencies and Stokes shifts (cm^{-1}) of the CENU derivatives investigated in different solvents.

CENU derivative	PNU			2FPNU			2MPNU			2MOPNU		
ν_x (cm^{-1})	ν_{abs}	ν_{em}	$\Delta\nu$	ν_{abs}	ν_{em}	$\Delta\nu$	ν_{abs}	ν_{em}	$\Delta\nu$	ν_{abs}	ν_{em}	$\Delta\nu$
Water	37,174	27,855	9319	37,174	27,932	9242	37,174	27,624	9550	37,037	28,089	8948
Methanol	37,313	28,248	9065	37,313	28,409	8904	37,593	27,932	9661	37,593	27,027	10,566
Ethanol	37,174	28,248	8926	37,313	28,571	8742	37,735	28 169	9566	37,735	28,248	9487
2-propanol	37,593	28,169	9424	37,313	28,571	8742	38,167	28,089	10,078	37,878	28,011	9867
DMSO	37,593	28,089	9504	37,453	27,548	9905	37,313	27,322	9991	37,313	27,548	9765
DMF	37,313	27,932	9381	37,174	27,247	9927	37,453	27,173	10,280	37,735	27,855	9880
Acetonitrile	37,593	27,932	9661	37,313	27,322	9991	37,313	27,322	9991	37,313	26,809	10,504
Acetone	37,453	27,932	9521	37,735	27,700	10,035	37,878	27,472	10,406	37,453	27,624	9829
DCM	37,174	27,173	10,001	37,313	27,855	9458	37,593	27,173	10,420	37,453	27,472	9981
EA	37,593	27,247	10,346	37,593	27,855	9738	37,735	27,322	10,413	36,900	27,322	9578
THF	37,593	27,472	10,121	37,735	28,089	9646	38,314	27,100	10,066	37,174	27,173	10,001
Cyclohexane	37,878	28,409	9469	38,022	27,548	10,474	37,453	27,397	10,056	37,593	27,472	10,121

Table S1 displays the solvent parameters [36–38] used in the multiple regression analysis fit. In order to dissect various solvent-specific effects, the solvatochromic analysis of the CENU derivatives was separately performed with all solvents, polar solvents only (water, methanol, ethanol, 2-propanol, DMSO, DMF, acetonitrile and acetone), and aprotic non-HBD solvents only (DMSO, DMF, acetonitrile, acetone, DCM, EA; THF and cyclohexane).

3.3.1. Multiparametric approach of Kamlet-Taft

Non-specific and specific solvent–solute interactions effects on absorption and emission spectra and Stokes shift of the investigated CENU derivatives were interpreted by a LSER using the following Kamlet-Taft equation [39]:

$$\nu_x = \nu_x^0 + p\pi^* + a\alpha + b\beta \quad (1)$$

where ν_x and ν_x^0 are the solvent-dependent property and the regression value of this solvent-dependent property in a reference solvent, respectively. The index of solvent dipolarity/polarizability, π^*, quantifies the ability of the solvent to stabilize a charge or a dipole by virtue of its dielectric effect. The measure of the solvent hydrogen-bond donor (HBD) acidity, α, illustrates the ability of a solvent to donate a proton in a solvent-to-solute hydrogen bond. The measure of the solvent hydrogen-bond acceptor (HBA) basicity, β, illustrates the solvent's ability to accept a proton (or, vice versa, to donate an electron pair) in a solute-to-solvent hydrogen bond. The regression coefficients *p*, *a*, and *b*, in Eq. 1, estimate the relative susceptibilities of the solvent-dependent solute property ν_x to the indicated solvent parameters [38]. This LSER has been extensively used in the modelling of solvation effects [6,40].

The results collected in Table S2 are obtained from the fit of the multiple regression analysis of the absorption and emission energies and Stokes shift employing Eq. 1 and data in Tables 3 and S1 (a). Plots of obtained calculated data according to Eq. 1, $\nu_{x\ calc.}$, versus the corresponding experimental data, $\nu_{x\ exp.}$, presented on Fig. 2 are used to check the success of the quantification and interpretation of solvent effects on the shifts of the absorption and emission maxima and Stokes shift of examined molecules.

Overall, the Kamlet-Taft model revealed mostly moderate linear correlations when all solvents (see Fig. 2a to c and r = 0.448–0.945 in Table S2) and when only aprotic solvents (see Fig. 2a'' to c'' and r = 0.161–0.859 in Table S2) were considered, whereas better correlations were obtained for polar solvents only (see Fig. 2a' to c' and r = 0.582–0.998 in Table S2). A possible reason for the partly significant deviations from linearity is that the Kamlet-Taft model does not consider potential steric interactions of substituents at the ortho position and/or the presence of intramolecular hydrogen bonds [6].

The key result of the solvatochromic analysis includes the susceptibility constants *p*, *a*, and *b*, which present a measure for the influence of each solvent parameter on the spectral property. To facilitate the evaluation of the different contributions of the solvent parameters on the spectroscopic properties, a "percentage contribution" is also established on the basis of the absolute values of *p*, *a*, and *b* (for example: $\pi^*\ \% = |p|/(|p| + |a| + |b|)$ such that $\pi^*\ \% + \alpha\ \% + \beta\ \% = 100\%$).

Quantification of solute–solvent interactions, from the absorption and emission bands and Stokes shifts, by the Kamlet-Taft solvatochromic comparison method shows that not only the polarity of the medium but also the hydrogen-bonding properties of the solvent affect the solvatochromic behavior of the investigated CENU derivatives.

Specifically, the solvatochromic contribution of the solvent dipolarity/polarizability (π^*) to the position of the absorption maximum, ν_{abs}, was $\geq$ 40% for all CENUs except for 2MOPNU in aprotic solvents (25%), and the sensitivity of electron-rich 2MPNU and 2MOPNU towards the HBA ability (β) was higher than to the HBD ability (α) of the solvent, whereas electron-poor 2FPNU and unsubstituted PNU appeared to be more sensitive to α than to β. The mostly negative sign of the *p* and *a* coefficients indicate a bathochromic shift of the absorption maximum with an increase in π^* and α for all CENUs, whereas PNU, 2MPNU and 2MOPNU show a hypsochromic shift with increasing β. This suggests a stabilization of the electronic excited state relative to the ground state except for these three CENUs in solvents with strong HBA ability.

The position of the emission maximum, ν_{em}, of all CENUs was also largely dependent on the solvent dipolarity/polarizability (π^*) exceeding 30% contribution in most cases and a negative sign of the *p* coefficient. The exception was 2MOPNU, which had a contribution of $\leq$25%, and a positive *p* coefficient indicating a hypsochromic shift of the emission maximum with an increase in π^*. Interestingly, the dependence on the HBA and HBD ability of the solvent appeared to be reversed in comparison to the absorption maximum. The sensitivity of electron-rich 2MPNU and 2MOPNU towards the HBA ability (β) appeared equal to or lower than to the HBD ability (α) of the solvent, whereas electron-poor 2FPNU and unsubstituted PNU appeared to be less sensitive to α than to β or similarly sensitive. The mostly positive sign of the *a* and *b* coefficients for all CENU derivatives except in aprotic solvents demonstrates a hypsochromic shift with increases in both, solvent HBD and HBA ability.

In view of the contrasting results for the solvatochromic effects on the absorption and emission maxima in different solvents, the dependence of the Stokes shift, $\Delta\nu$, on the solvent parameters was less clear. Overall, it appears that the Stokes shift decreases for the three most electron-poor 2FMPNU, PNU, and 2MPNU with increasing HBD and HBA ability (negative sign for *a* and *b*).

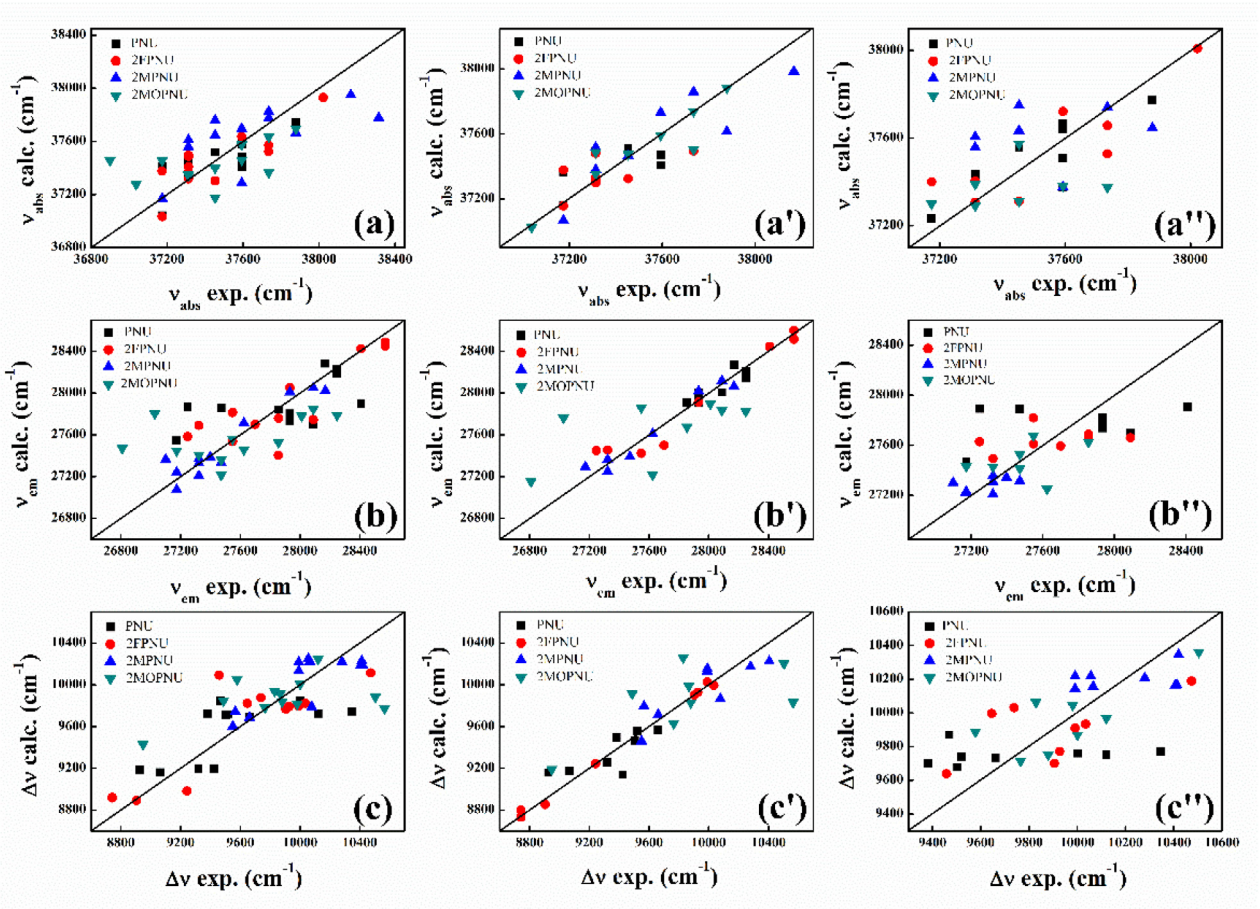

Fig. 2. Kamlet-Taft LSER plots of the calculated values of (a) ν_{abs}, (b) ν_{em}, and (c) Δν plotted against the corresponding experimental data in all solvents (no prime), polar solvents ('), and aprotic solvents (").

3.3.2. Multiparametric approach of Catalán

Catalán [36] proposed a refinement of the Kamlet-Taft model by splitting the solvent dipolarity/polarizability parameter, π*, into solvent polarizability (SP) and solvent dipolarity (SdP) parameters according to Eq. 2:

$$A = A_0 + sSP + dSdP + aSA + bSB \quad (2)$$

where SP is the solvent polarizability, SdP is the solvent dipolarity, SA is the solvent's hydrogen bond donor strength and SB is the solvent's hydrogen bond acceptor strength. *s*, *d*, *a* and *b* are the regression coefficients. Thus, the contribution of Catalán's parameters to the absorption and emission frequencies and Stokes shift of the CENU derivatives could be estimated.

The results of the Catalán model (Fig. 3 and Table S3) were generated from the fit of the multiple regression analysis of the absorption and emission energies and Stokes shift using Eq. 2 and the data in Tables 3 and S1 (b). As it can be observed from Fig. 3 and from the *r* values in Tables S2 and S3, the multilinear analysis of ν_{abs}, ν_{em} and $\Delta\nu$ data according to the Catalán equation produced the same quality of correlation between the predicted and experimental spectroscopic properties as the Kamlet-Taft model for all CENU derivatives investigated in all solvents (see Fig. 3d to f and r = 0.421–0.878 in Table S3), in aprotic solvents (see Fig. 3d" to f" and r = 0.365–0.929 in Table S3), and in polar solvents only (see Fig. 3d' to f' and r = 0.565–0.980 in Table S3). As in the Kamlet-Taft model, the deviations from linearity might be ascribed to steric interactions of substituents at ortho position and/or the presence of intramolecular hydrogen bonding, which both, the Catalán and the Kamlet-Taft equations, do not take into account [6]. Nonetheless, the satisfactory correlations of absorption and emission maxima as well as the Stokes shift indicate that the Catalán model gives also a correct interpretation of LSER of the investigated CENU derivatives in the solvents used.

Gratifyingly, the main results from the LSER according to the Catalán equation agreed with the results from the Kamlet-Taft analysis. The solvatochromic contribution of the solvent polarity parameters, solvent polarizability (SP) and solvent dipolarity (SdP), to the position of the absorption and emission maxima was significant for all CENUs (combined ≥ 45%) except for aprotic solvents only. The Catalán analysis additionally revealed larger contributions of the polarizability for electron-poor 2FPNU and unsubstituted PNU and larger contributions of the dipolarity for electron-rich 2MPNU and 2MOPNU to the overall solvent polarity effect. Also, the higher sensitivity of the absorption maxima of electron-rich 2MPNU and 2MOPNU towards the HBA ability (SB) than to the HBD ability (SA) of the solvent, the reversed behavior for electron-poor 2FPNU and unsubstituted PNU, as well as the reversal of this trend in the emission maxima was clearly confirmed by the Catalán model when polar solvents were not excluded from the analysis. Moreover, the general trend for the regression coefficients *s*, *d*, *a* and *b* obtained by the Catalán model was in accordance with the respective coefficients *p*, *a*, and *a* from the Kamlet-Taft model.

3.3.3. Multiparametric approach of Laurence

Laurence et al. have recently modified the LSER by introducing new parameters [33,37]:

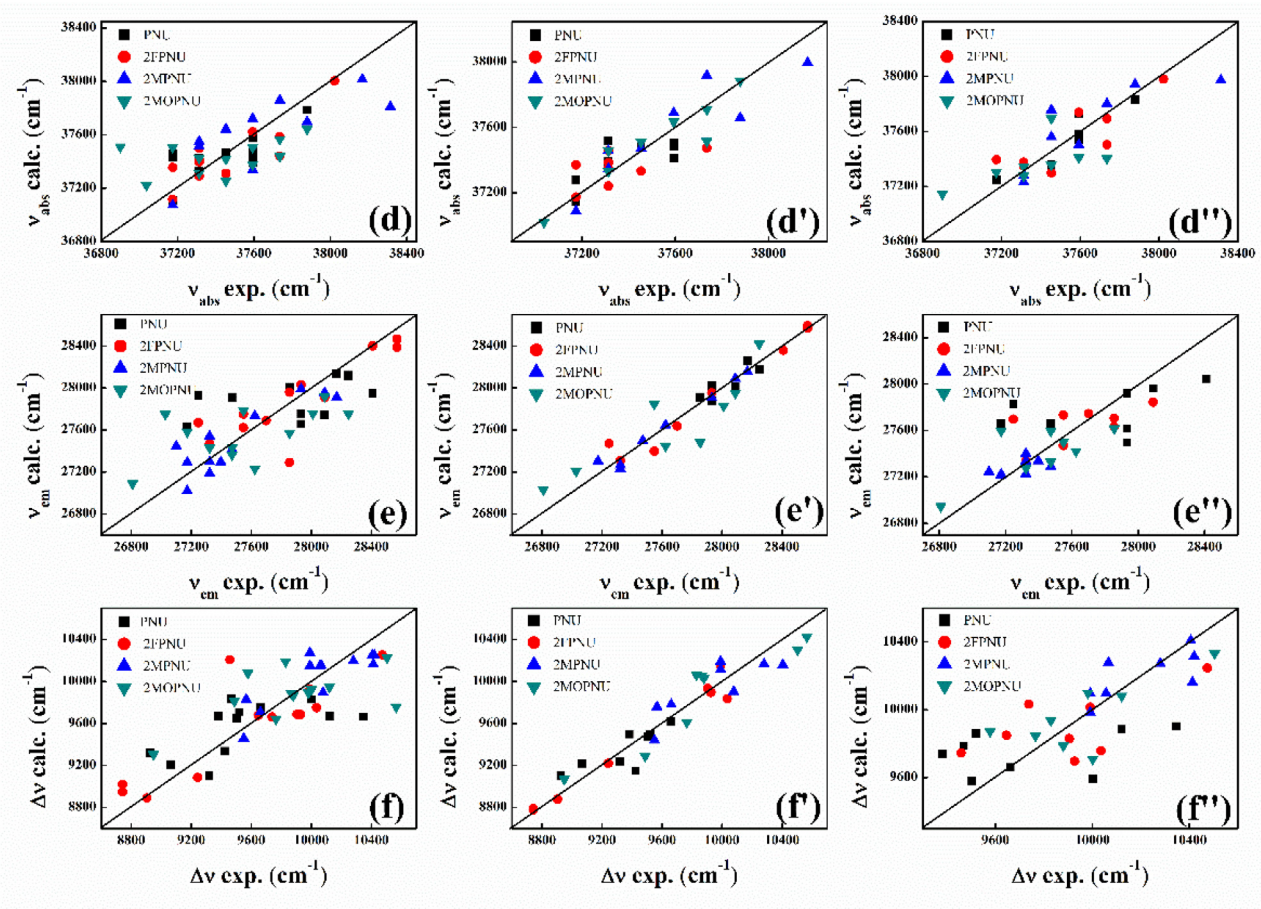

Fig. 3. Catalán LSER plots of the calculated values of (d) ν_{abs}, (e) ν_{em}, and (f) $\Delta\nu$ versus their corresponding experimental data in all solvents (no prime), polar solvents ('), and aprotic solvents (").

$$\nu_a = \nu_0 + di\mathrm{DI} + e\mathrm{ES} + a\alpha_1 + b\beta_1 \quad (3)$$

where DI are dispersion and induction interactions, ES the electrostatic interactions between permanent dipoles of the solute and the solvent, and α_1 and β_1 the HBD and HBA ability of the solvent, respectively, where α_1 and β_1 have the same meaning as the respective solvent parameter values in the Kamlet-Taft and Catalán models. The symbols *di*, *e*, *a*, and *b* represent the corresponding regression coefficients.

The multiple linear regression analysis of the photophysical properties in Table 3 with the solvent parameters in Table S1 (c) with the Laurence equation Eq. 3, yields the results in Fig. 4 and the calculated values displayed in Table S4. The correlation coefficients *r* obtained with the Laurence model (Table S4) displayed the same quality of correlation between the predicted and experimental spectroscopic properties as the Kamlet-Taft (Table S2) and Catalán model (Table S3) for all CENU derivatives investigated in all solvents (see Fig. 4g to i and *r* = 0.186–0.852 in Table S4) and in aprotic solvents (see Fig. 4g" to i" and *r* = 0.304–0.912 in Table S4), whereas the correlation in polar solvents only was clearly better with the Laurence model and consistently ≥ 0.849 for the emission maximum and Stokes shift (see Fig. 4h' and i' and Table S4).

In general, the trends from the Kamlet-Taft and Catalán models seem to be reflected in the regression coefficients obtained with the Laurence model. For example, the Kamlet-Taft and Catalán analysis consistently indicated that the contributions from the HBA and HBD ability of the solvent do not exceed 70% and that the solvent polarity parameters contribute more than 30% to the solvatochromic shifts of the absorption and emission maxima, which is also confirmed with the Laurence model. However, the dependence of the absorption and emission maxima of the electron-rich 2MPNU and 2MOPNU compared to the electron-poor 2FPNU and unsubstituted PNU became not apparent in the regression coefficients obtained with the Laurence model, not even in the best correlated data. This indicates that the Laurence model may not provide a correct interpretation of LSER of CENU derivatives in the solvents used, although similar limitations as for the Kamlet-Taft and Catalán model have been noted [6].

3.3.4. Discussion of the solvatochromism of the CENU derivatives

Overall, it was found that the solvent dependence of the absorption and emission maxima of the CENU derivatives was satisfactorily correlated with the solvent parameters of all three solvatochromic models. The dissection of the single parameter π^* for non-specific solvent effects in the Kamlet-Taft equation into dipolarity, SdP, and polarizability, SP, in the Catalán model or into dispersion and induction interactions, DI, and electrostatic interactions, ES, in the Laurence model did not significantly improve the quality of the correlations.

The multiparametric analysis of the data collected in Tables S2 to S4 indicated that most of the solvatochromic effects on the absorption and emission maxima are attributed to both, non-specific solute–solvent interactions (to generally > 30%) and specific solute–solvent interactions, i.e. the solvent's HBD and HBA ability (to generally < 70%). This is in accordance with the structure of all investigated CENU derivatives, which indicate the possibility for hydrogen bonding with the solvent due to the presence of hydro-

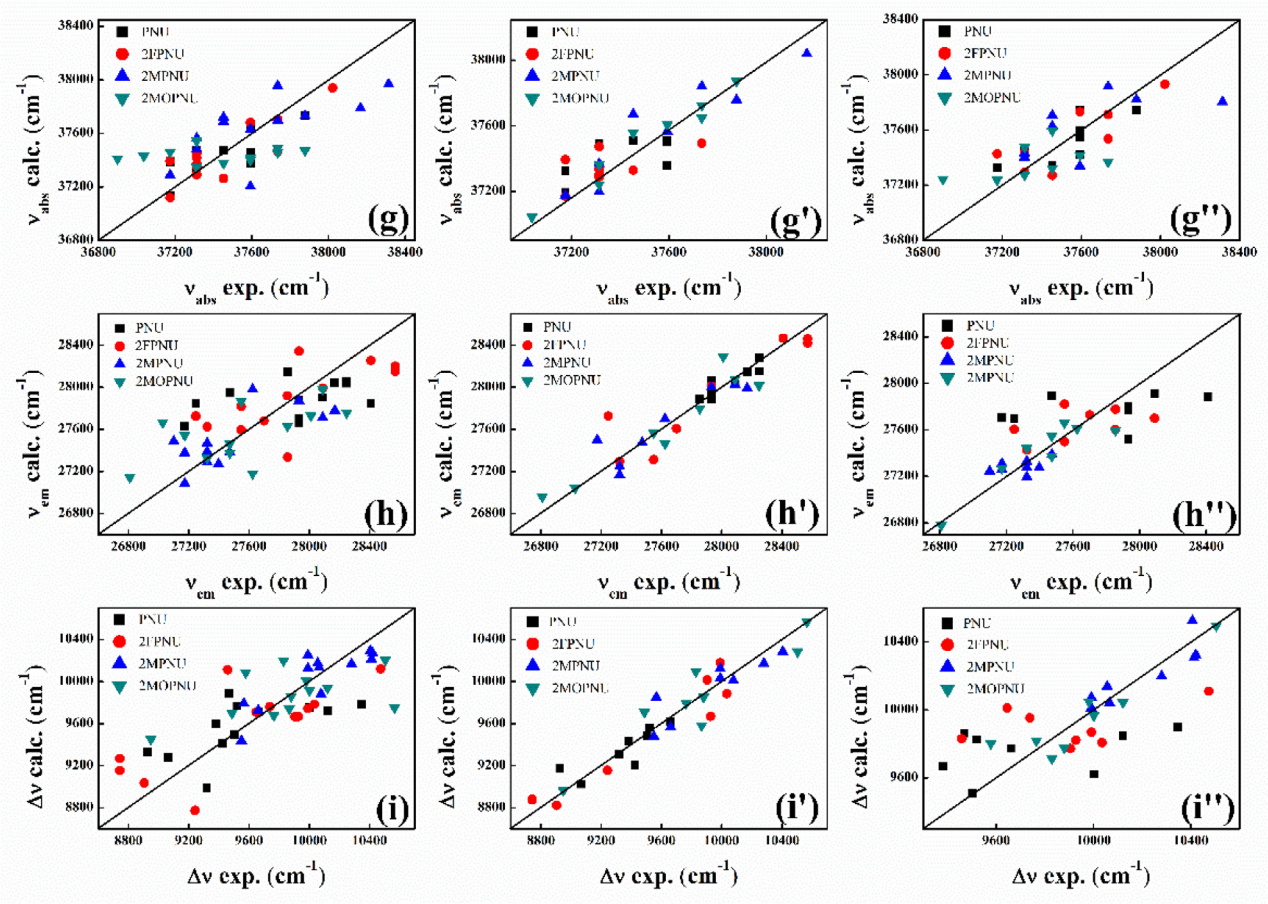

Fig. 4. Laurence LSER plots of the calculated values of (g) ν_{abs}, (h) ν_{em}, and (i) $\Delta\nu$ versus their corresponding experimental data in all solvents (no prime), polar solvents ('), and aprotic solvents (").

gen bond-accepting (carbonyl C=O, nitroso N=O) and hydrogen bond-donating groups (amide N-H).

Interestingly, we found in the multiparametric analysis using the Kamlet-Taft and Catalán models that the contribution of the parameter reflecting the HBA ability (β and SB) of the solvent to the solvatochromic shift of the absorption maximum, ν_{abs}, of the electron-poor CENUs, PNU and 2FPNU, is unexpectedly small. The low sensitivity of the two CENU derivatives to the hydrogen bond basicity of the medium may be explained by the possible existence of an intramolecular hydrogen bond N=O...HN in PNU and 2FPNU (Fig. S3), which would effectively prevent the formation of hydrogen bonds of the urea N-H with a hydrogen bond-accepting solvent [5,6]. In contrast, the sensitivity of the electron-rich CENUs, 2MPNU and 2MOPNU, to the HBA ability of the medium is more pronounced, in particular when aprotic solvents are excluded from the Catalán model, indicating that the intramolecular hydrogen bond is significantly weakened or even absent in 2MPNU and 2MOPNU.

It is also interesting to note that the position of the emission maximum, ν_{em}, of all CENUs are more dependent on the HBA ability of the solvent than the absorption maxima. This indicates that the intramolecular hydrogen bond may be significantly loosened in the excited state. This interpretation is in accordance with the observation that the emission maxima of the electron-poor PNU and 2FPNU are more dependent on the HBA ability of the solvent than on the HBD ability, whereas the electron-rich 2MPNU and 2MOPNU are equally dependent on HBA and HBA ability.

The degree of intramolecular hydrogen bonding is, apparently, influenced by the electron density on the nitrogen atom of the amino group, which is influenced by the nature of the substituent in the aromatic ring (substituents with an electron-donating effect weaken the intramolecular hydrogen bonding while substituents with an electron-withdrawing effect strengthen the intramolecular hydrogen bonding). Furthermore, where the strength of the intramolecular bonding is small, it is expected that the influence of intermolecular hydrogen bonding is large [41]. This interpretation is in line with a steric hindrance and/or the electron-donating effect caused by the *ortho*-methoxy and *ortho*-methyl groups. Noteworthy, a steric effect influences the interaction with all the solvents to the same extent, while intramolecular hydrogen-bonding influences the interaction with the protic solvents more than with the aprotic solvents [42]. Hence, the absorption and emission spectra and Stokes shift of the examined CENU derivatives are mainly dependent on the polarity of the solvents, whereas the detailed solvatochromic response is dependent on the exact chemical structures of the chromophores and the solvents.

Besides, the presence of an aromatic group is expected to confer all CENU derivatives a pronounced solvent polarity. This is nicely confirmed by the data in Tables S2 to S4, which shows that the general solvent effects display a predominant influence on the solvatochromic shifts of the investigated CENU derivatives.

3.4. Solvent effect on the structure-activity relationship

It is well known that the molecular structure and the physicochemical properties governs the interactions of drug molecules with their environment and, thus, have a major influence on their behavior in biological processes of the human body. Since the sol-

vatochromism of the investigated CENU derivatives similarly reflects their interactions with the surrounding solvent molecules, we speculated whether relationships between polarity and hydrogen bonding interactions as revealed by the solvatochromic analysis and selected structural properties related to the ADME parameters could be established.

Therefore, the regression coefficients obtained from LSER with the Catalán model from absorption frequencies (from all solvents, polar, and aprotic solvents tested, respectively) were used and the estimated ADME parameters (HIA, Caco-2, MDCK, BBB penetration and PPB property) were plotted against (|*s*|+|*d*|), i.e., the sum of the absolute values of the regression coefficients of the solvent polarizability (SP) and the solvent dipolarity (SdP), respectively. The latter were thought to serve as a measure of the importance of non-specific interactions.

This analysis revealed acceptable linear dependencies (Table 4, r^a values) between the solvatochromic regression coefficients and some ADME parameter suggesting correlations between the different ADME parameters and non-specific solute–solvent interactions. In particular, a very good correlation was found between the BBB permeation (r = 0.997 for polar solvents) and non-specific solvent–solute interactions as expressed by (|*s*|+|*d*|). Since the ability of a molecule to permeate across a cell membrane is mostly influenced by the hydrophilicity/lipophilicity balance it is reasonable that the non-specific interactions to overall solvation effects are correlated with lipophilicity and thus increase the permeation [31]. Similarly, an increased lipophilicity should also show a good correlation with unspecific protein binding expressed as PPB, which was, in fact, observed (r = 0.999 for aprotic solvents). In view of this, it is intriguing to see that the correlation with HIA, Caco-2 and MDCK absorption parameters was, at best, moderate (with r < 0.80), whereas the correlation with BBB permeation was very high (Table 4, r^a values).

It was further attempted to include (|*a*|+|*b*|) from the absorption frequencies of the Catalán model in the correlation with the ADME parameters, which is the sum of the absolute values of the regression coefficients of the solvent's hydrogen bond donor strength, SA, and the solvent's hydrogen bond acceptor strength, SB. This significantly improved all correlations (Table 4, r^b values). In particular the correlation coefficients between the HIA, Caco-2 and MDCK permeabilities and the regression coefficients in polar solvents increased dramatically to r = 0.890, 0.897, and 0.974, which clearly suggests that the hydrogen bond interactions are the main contributors in governing HIA, Caco-2 and MDCK absorption properties.

In summary, these correlations confirm the importance of the relative contributions from the non-specific and specific solute–solvent interactions on ADME parameters of CENU derivatives. They may even pave the way for generating new equations that demonstrate exact relationships between solute–solvent interactions and structure–activity parameters.

3.5. Effect of β-CD complexation

Since the CENU derivatives investigated were found to be sensitive to the surrounding environment (polarity, dipolarity, polarizability, HBD and HBA strengths), changes of the spectroscopic properties can also be used to follow encapsulation into CD cavity. Therefore, the complexation was followed by spectrofluorometry in acetonitrile [6] and the fluorescence spectra of the four investigated CENU derivatives with increasing concentrations of β-CD are shown in Fig. 5.

Inclusion of a fluorescent guest into a supramolecular host changes the spectral properties of the guest and the most common outcome for CDs is fluorescence enhancement. This can be attributed to protection against collisional quenching, changes in the microenvironment, or a decreased flexibility of the guest due to confinement in the host cavity [43]. Most prominent is the relocation from a more hydrophilic environment (most often water) into the hydrophobic environment of the CD cavity.

We can deduce, from the fluorescence spectra of the investigated CENU derivatives in Fig. 5, that the addition of increasing concentrations of *β*-CD causes significant increase in their fluorescence emission intensities with significant changes in the position of the emission maxima, where red shifts of 4, 4, 4 and 10 nm for PNU, 2FPNU, 2MPNU and 2MOPNU, respectively, of the original peak positions were observed. Since we have established above that the shift of the maximum emission wavelength is sensitive towards a change in the environment surrounding the fluorophore, the red shift represents a clear indication for binding with the CD cavity. We propose complex formation between β-CD and each CENU derivative, in which each of the investigated CENU derivatives is included, or at least partially included, into the β-CD cavity in acetonitrile solutions.

The stoichiometry and the corresponding binding constants of the inclusion complexes of the four CENU derivatives with β-CD were assessed using Benesi-Hildebrand relations as expressed by Eqs. (4) and (5) [44]. In the case that only the 1:1 complexes are formed, the binding constants' values for the formation of 1:1 complexes, can be calculated based on the following Benesi-Hildebrand relation [44]:

$$\frac{1}{I - I_0} = \frac{1}{(I_1 - I_0)} + \frac{1}{(I_1 - I_0)K_1[CD]} \tag{4}$$

where I_0, I and I_1 are the fluorescence intensities of the fluorophores without β-CD, with a particular concentration of β-CD, and at the maximum concentration of β-CD used, respectively, [*CD*] is the total concentration of β-CD molecule added during the titration, and K_1 represents the binding constant for 1:1 complex formation.

For 2:1 (host:guest) inclusion complexes, the following Benesi-Hildebrand relation [44] can be used:

$$\frac{1}{I - I_0} = \frac{1}{(I_1 - I_0)} + \frac{1}{(I_1 - I_0)K_1K_2[CD]^2} \tag{5}$$

Table 4
Correlation between the ADME parameters and the sum of the regression coefficients from Catalán model, for the investigated CENU derivatives.

ADME parameter		HIA	Caco-2	MDCK	BBB	PPB
All solvents tested	r^a	0.122	0.243	0.140	0.675	0.100
	r^b	0.789	0.626	0.956	0.697	0.275
Polar solvents	r^a	0.520	0.569	0.326	0.997	0.792
	r^b	0.890	0.897	0.974	0.999	0.802
Aprotic solvents	r^a	0.795	0.599	0.536	0.805	0.999
	r^b	0.808	0.664	0.610	0.931	0.999

r^a : Correlation coefficient, *r*, between the ADME parameters and the sum of the regression coefficients (|*s*|+|*d*|) obtained from the solvatochromic analysis of the absorption maxima with the Catalán model.
r^b : Correlation coefficients, *r*, between the ADME parameters and the sum of the regression coefficients (|*s*|+|*d*|) and (|*a*|+|*b*|) from the absorption maxima of the solvatochromic analysis with the Catalán model.

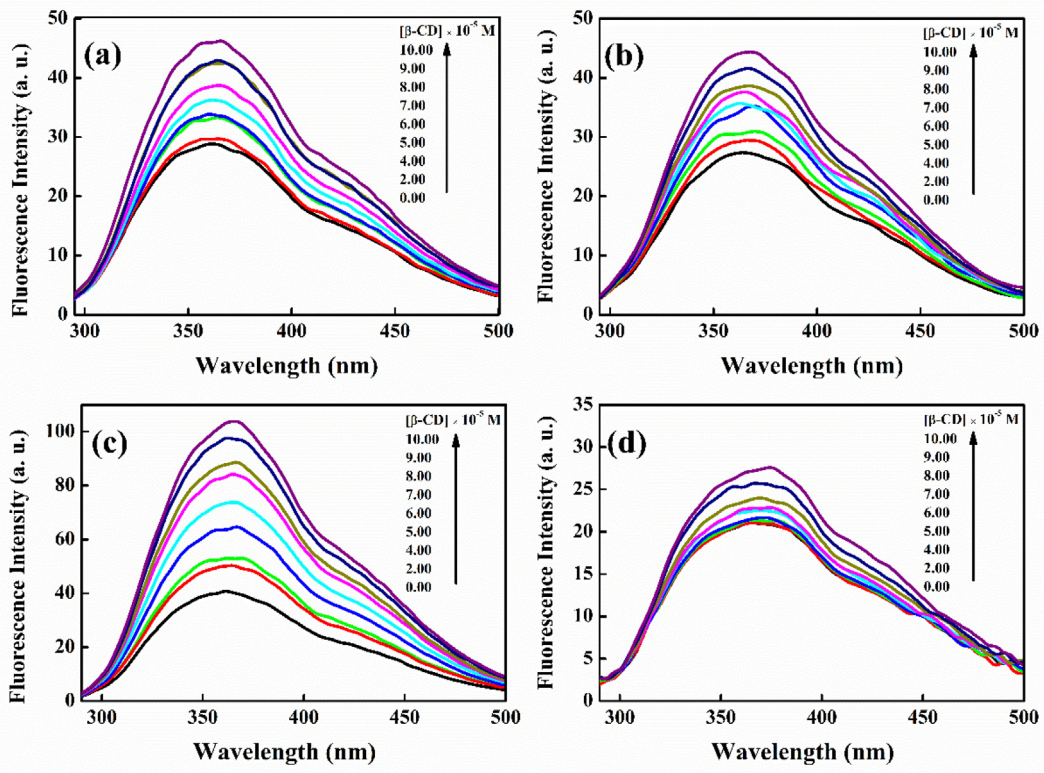

Fig. 5. Emission enhancement of the investigated CENU derivatives : (a) PNU, (b) 2FPNU, (c) 2MPNU and (d) 2MOPNU in presence of increasing concentrations of β-CD. [CENU] = 1.00 × 10^{-5} M; [β-CD] = 0–10.00 × 10^{-5} M.

where K_2 represents the binding constant for the second step of the 2:1 complex formation.

Benesi-Hildebrand plots yielded straight lines with excellent linear regressions (r = 0.974, 0.982, 0.987 and 0.981, respectively) for 1:1 (host:guest) inclusion complexes (Fig. 6), whereas no linear relationship was obtained for the $1/(I - I_0)$ versus $1/[CD]^2$ plots (Fig. 7). This confirms the supposed 1:1 β-CD:CENU inclusion complexes and rules out the possibility of forming 2:1 inclusion complexes between β-CD and each CENU derivative. The experimental binding affinities, K_1, were 1316, 600, 2200 and 5071 M^{-1} for the CD-PNU, CD-2FPNU, CD-2MPNU and CD-2MOPNU complexes, respectively.

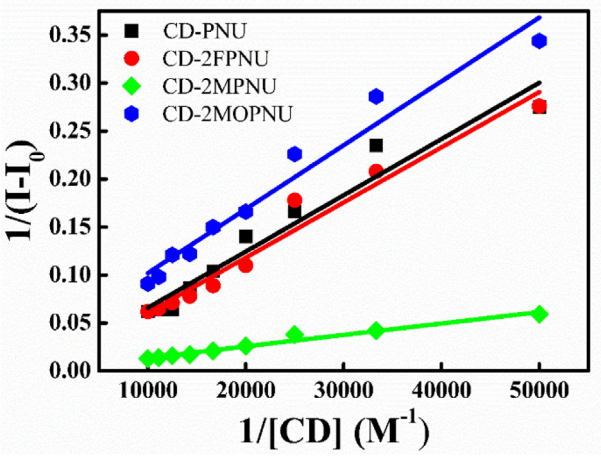

Fig. 6. Benesi-Hildebrand plots for the 1:1 inclusion complexes.

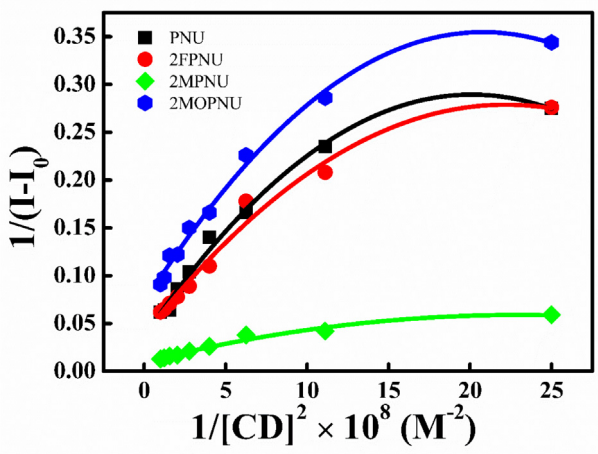

Fig. 7. Benesi-Hildebrand plots for the 2:1 inclusion complexes.

The binding stoichiometry of β-CD-CENU inclusion complexes was further confirmed by the continuous variation method [45] and the molar ratios method [46]. According to continuous variation method, equimolar (1.00 × 10^{-5} M) solutions of each CENU derivative and β-CD were prepared and mixed to afford varying molar fractions of β-CD (between 0.20 and 0.80), while the total concentration of the species ([β-CD] + [CENU]) was kept constant. After stirring, the emission was measured for all solutions and the fluorescence intensity (FI) was plotted as a function of the [β-CD]/([β-CD] + [CENU]) ratio. In Fig. 8 are presented Job's plots, showing maxima at a molar fraction of 0.5, indicating that the stoichiometry of the complexes is 1:1.

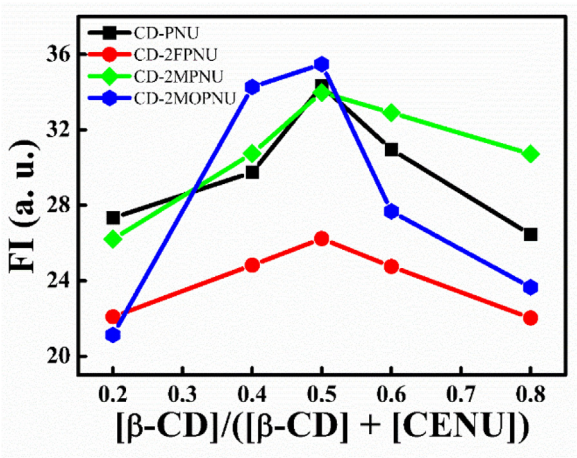

Fig. 8. Continuous variation plots.

In the molar ratios method, the FI is expressed as a function of [β-CD]/[CENU] ratio. Therefore, equimolar stock solutions of CENU and β-CD were prepared (1.00×10^{-5} M) and varying volumes of the β-CD stock solution (from 0.4 to 6 mL) were mixed with a fixed volume (2 mL) of the CENU solution. This gave solutions with identical total concentration of the two species, β-CD and each CENU derivative (1.00×10^{-5} M), while the molar ratio [β-CD]/[nitrosourea] was varied from 0.2 to 3. From the molar ratios method, the abrupt variations of the slopes in plots FI against molar ratios [β-CD]/[CENU] at about 1:1 mol ratio, as shown in Fig. 9, indicates the formation of 1:1 inclusion complexes and confirmed the formation of an association between β-CD and CENU with a 1:1 M ratio of β-CD to CENU.

The binding constant, K_1, reflects the strength of the binding interactions of β-CD with guest molecules and, in the case of CENU derivatives, relatively high affinities and a certain selectivity were obtained. The large binding constant values of some β-CD-CENU complexes demonstrate efficient complexation of the drug molecules with β-CD, whereas the inclusion interactions of β-CD and the investigated CENU derivatives can be affected by many factors. It is generally believed that the driving forces involved in the formation of CD inclusion complexes include electrostatic interactions, van-der-Waals forces, hydrophobic interactions, and hydrogen bonding, which cooperatively govern the stability of the inclusion complex. The relative importance of each of these contributions depends on the properties of the specific guest being included [47]. For the CENU derivatives, the binding affinity to β-CD is in the order 2MOPNU > 2MPNU > PNU > 2FPNU.

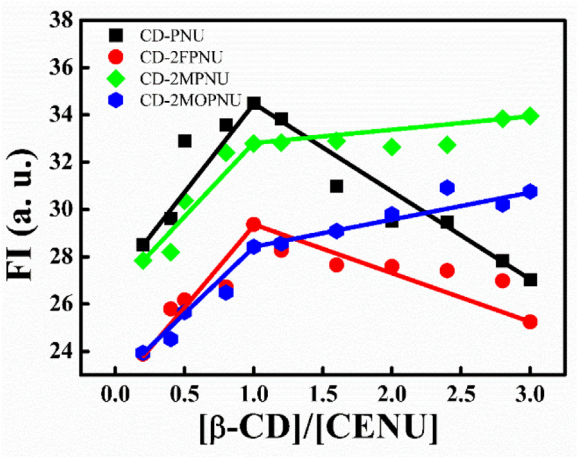

Fig. 9. Molar ratios plots.

Commonly, the major driving force for β-CD complexation in water is the hydrophobic effect, which enables hydrophobic drug molecules to bind to the hydrophobic CD cavity. Since our studies have been performed in acetonitrile as a solvent, a major contribution from the hydrophobic effect is thus less likely. Potential other contributions to the observed affinity and selectivity originate from hydrogen bonding of the guest with primary or secondary hydroxyl groups of β-CD or from van-der-Waals interactions. Very reasonable is also a contribution from C-H-π interactions between the inner cavity hydrogen atoms with the highly polarizable aromatic rings of the CENU derivatives.

The binding selectivity clearly correlates with the electron density of the aniline ring, such that the CENU derivative with the highest electron density (2MOPNU carrying an *ortho*-methoxy group) binds strongest and the CENU derivative with the lowest electron density (2FPNU with an *ortho*-fluorine group) binds weakest. This is well in line with increased van-der-Waals and C-H-π interactions of the electron-rich CENU derivatives. A contribution from steric crowding, which disfavors the complexation, is not observed since the most bulky *ortho*-methoxy-substituted CENU derivative binds strongest.

4. Conclusion

A new series of four potential anticancer agents derived from CENU was synthesized. The ADME/Tox prediction study revealed that the investigated CENU derivatives can be good candidates as anticancer agents for CNS-related cancers with high probability of crossing the BBB. The contribution of specific and non-specific solvent interactions to the observed solvatochromic behavior was quantitatively evaluated with the multiparametric Kamlet-Taft solute–solvent interaction model, which revealed the dependence of the solvatochromic behavior of the investigated CENU derivatives on both, the polarity of the medium and the hydrogen-bonding properties of the solvent. Furthermore, the application of Catalàn and Laurence models has shown that the non-specific interactions are the main factors contributing to the solvatochromism exhibited by the investigated CENU derivatives. It was also shown that the solvatochromic properties of these substituted CENU derivatives are influenced by the type of substituent. The evidence for solvation effects on the structure–activity relationship of the investigated molecules was obtained by correlating HIA, Caco2, MDCK, BBB and PPB parameters with the contributions of non-specific and specific solute–solvent interactions, demonstrating satisfactory relationships between solute–solvent interactions and structure–property parameters. Based on spectrofluorimetric analysis, binding constant values and stoichiometries for the inclusion complexes between β-CD and each CENU derivative were evaluated. Both methods, the continuous variation and the molar ratios method, support the formation of 1:1 inclusion complexes. We have found that many factors highly influence the inclusion complexation of guest CENU derivatives with β-CD, including simultaneously, the hydrophobicity and substituent effect of the guest, which determine the stability of host–guest complexes through the hydrophobic and hydrogen-bonding interactions.

In view of these points, it is reasonable to propose that, studying CENU derivatives' spectral properties under different conditions will lead to better explaining their biological activities and better development of anticancer CENU drugs.

CRediT authorship contribution statement

Hassina Fisli: Investigation, Formal analysis, Writing - original draft. **Andreas Hennig:** Conceptualization, Writing - review & edit-

ing, Visualization. **Mohamed Lyamine Chelaghmia:** Validation, Visualization. **Mohamed Abdaoui:** Supervision.

Declaration of Competing Interest

The authors declare that they have no known competing financial interests or personal relationships that could have appeared to influence the work reported in this paper.

Acknowledgements

We are very grateful to the financial support within the general direction of scientific research and technology development of the Algerian ministry of higher education and scientific research.

Appendix A. Supplementary material

Supplementary data to this article can be found online at https://doi.org/10.1016/j.saa.2021.119579.

References

[1] a. Diksic, M., Sako, K., Feindel, W. et al. Pharmacokinetics of positron-labeled 1,3-Bis(2-chloroethyl)nitrosourea in human brain tumors using positron emission tomography. Cancer Res. 44 (1984) 3120-3124; b. J. W. Lown, , S. M. S.Chuhan, Synthesis of specifically nitrogen-15- and carbon-13-labeled antitumor (2-haloethyl)nitrosoureas. The study of their conformations in solution by nitrogen-15 and carbon-13 nuclear magnetic resonance electronic control in their aqueous decomposition. J. Org. Chem. 46, 26 (1981) 5309-5321; c. J. W. Lown, S. M. S.Chuhan, Mechanism of action of (2-haloethyl) nitrosoureas on DNA. Isolation and reactions of postulated 2-(alkylimino)-3-nitrosooxazolidine intermediates in the decomposition of 1,3-bis(2-chloroethyl)-, 1-(2-chloroethyl)-3-cyclohexyl-, and 1-(2-chloroethyl)-3-(4'-trans-methylcyclohexyl)-1-nitrosourea. J. Med. Chem. 24, 3 (1981) 270-279; d. J. W. Lown, S. M. S.Chuhan, Synthesis and reactions of deuterated 2-(alkylimino)-3-nitrosooxazolidines, 3-alkyl-1-(2-hydroxyethyl)-1-nitrosoureas, and related compounds as possible intermediates in the aqueous decomposition of 3-alkyl-1-(2-chloroethyl)-1-nitrosoureas. J. Org. Chem. 46, 12 (1981) 2479-2489; e. G. P. Wheeler, A Review of Studies on the Mechanism of Action of Nitrosoureas. Cancer Chemotherapy. Chap. 5 pp 87-119 ACS Symposium Series Vol. 30 (1976)

[2] C.T. Gnewuch, G. Sosnovsky, A critical appraisal of the evolution of N-nitrosoureas as anticancer drugs, Chem. Rev. 97 (3) (1997) 829–1013.

[3] K. Yano, H. Katayama, K. Takemoto, Interrelationship between Tumorigenicity and the Chemical Nature of A/-Methyl-AT-aryl-A/-nitrosoureas, Canc. Res. 44 (1984) 1027–1030.

[4] K. Yan, M. Isobe, Mutagenicity of N-Methyl-N'-aryl-N-nitrosoureas and N-Methyl-N'-aryl N'-methyl-N-nitrosoureas in Relation to Their Alkylating Activity, Cancer Res. 39 (1979) 5147–5149.

[5] H. Fisli, N. Bensouilah, N. Dhaoui, M. Abdaoui, Effects of solvent, pH and β-cyclodextrin on the fluorescent behaviour of lomustine, J. Incl. Phenom. Macrocycl. Chem. 73 (2012) 369–376.

[6] H. Fisli, N. Bensouilah, M. Abdaoui, Spectrofluorimetric determination of the antineoplastic agent lomustine based on the sensitizing effect of β-cyclodextrin, Luminescence 31 (3) (2016) 871–880.

[7] L.C. Panasci, D. Green, R. Nagourney, P. Fox, P.S. Schein, A structure-activity analysis of chemical and biological parameters of chloroethylnitrosoureas in mice, Cancer Res. 37 (1977) 2615–2618.

[8] F. Ali-Osman, J. Giblin, M. Berger, M.J. Murphy Jr, M.X. Rosenblum, Chemical structure of carbamoylating groups and their relationships to bone marrow toxicity and anti-glioma activity of bifunctionally alkylating and carbamoylatingnitrosoureas, Cancer Res. 45 (1985) 4185–4191.

[9] a. K. D. Gavlik, E. S. Sukhorukova , Y. M. Shafran, P. A. Slepukhin, E. Benassi, N. P. Belskaya,2-Aryl-5-amino-1,2,3-triazoles: New effective blue-emitting fluorophores. Dyes Pigm. 136 (2017) 229-242; b. P. Avouris, W.M. Gelbert, M.A. El-Sayed, Nonradiative electronic relaxation under collision-free conditions. Chem. Rev. 77 (1977) 793-833

[10] a. J. Kabatc, B. Jędrzejewska, P. Orliński, J. Pączkowski, The synthesis and the solvent and substituent effect on the spectroscopic characteristic of 3-ethyl-2-(p-substituedstyryl)benzothiazoliumiodides. Spectrochim. Acta A. 62 (2005) 115–125; b. T. Elsaesser, W. Kaiser, Vibrational and Vibronic Relaxation of Large Polyatomic Molecules in Liquids. Annu. Rev. Phys. Chem. 42 (1991) 83-107, and references therein

[11] A.C. Santos, D. Costa, L. Ferreira, C. Guerra, M. Pereira-Silva, I. Pereira, D. Peixoto, N.R. Ferreira, F. Veiga, Cyclodextrin-based delivery systems for in vivo-tested anticancer therapies. Drug Deliv, Transl. Res. (2020), https://doi.org/10.1007/s13346-020-00778-5, Published online: 21 May 2020.

[12] a. N. Erdoğar, E. Nemutlu, A. B. İskit, S. C. Kara, Z. Şafak Teksin, E. Bilensoy, Improved oral bioavailability of anticancer drug tamoxifen through complexation with water soluble cyclodextrins: in vitro and in vivo evaluation. J. Incl. Phenom. Macrocycl. Chem. 96 (2020) 81-91; b. H. Sadaquat, M. Akhtar, Comparative effects of β cyclodextrin, HP β cyclodextrin and SBE7 β cyclodextrin on the solubility and dissolution of docetaxel via inclusion complexation. J. Incl. Phenom. Macrocycl. Chem. 96 (2020) 333-351; c. A. Lodagekar, R. M. Borkar, S. Thatikonda, R. B. Chavan, V. G. M. Naidu, N. R. Shastri, R. Srinivas, N. Chella, Formulation and evaluation of cyclodextrin complexes for improved anticancer activity of repurposed drug: Niclosamide. Carbohydr. Polym. 212 (2019) 252-259; d. Szejtli, J.: Molecular entrapment and release properties of drugs by Cyclodextrin. In: Smolen, V.F., Ball, L.A. (eds.) Controlled drug bioavailability, vol. 3, pp. 365-420. Wiley, New York (1989); e. Szejtli, J.: Cyclodextrin Technology. Kluwer Academic Publishers, Dordrecht (1988); f. Szejtli, J.: Medicinal applications of cyclodextrins. Med. Res. Rev. 14, 3 (1994) 353-386; g. Szejtli, J.: Cyclodextrins and their inclusion complexes. AkademiaiKiado, Budapest (1982); h. Duchene, D.: Cyclodextrins and their industrial uses. Editions de Santé, Paris (1987); i. Szejtli, J., Osa, T.: ComprehensiveSupramolecularChemistry, Cyclodextrins, vol. 3. Elsevier, Oxford (1996)

[13] T. Looftsson, H. Fridriksdottir, Degradation of lomustine (CCNU) in aqueous solution, Inter. J. Pharm. 62 (1990) 243–247.

[14] E. Uria-Canseco, S. Perez-Casas, G. Navarrete-Vázquez, Thermodynamic characterization of the inclusion complexes formation between antidiabetic new drugs and cyclodextrins, J. Chem. Thermodyn. 129 (2019) 55–60.

[15] R.J. Flaherty, B. Nshime, M. DeLaMarre, S. DeJong, P. Scott, A.W. Lantz, Cyclodextrins as complexation and extraction agents for pesticides from contaminated soil, Chemosphere 91 (2013) 912–920.

[16] M. Kfoury, D. Landy, S. Fourmentin, Characterization of Cyclodextrin/Volatile Inclusion Complexes: A Review, Molecules 23 (2018) 1204–1227.

[17] M.V. Rekharsky, Y. Inoue, Complexation Thermodynamics of Cyclodextrins, Chem. Rev. 98 (1998) 1875–1917.

[18] , Determination of Stability Constants Vol. 8 (1996) 425–482.

[19] Chemical, Physical and Biological Aspects of Confined Systems, Vol. 1: Cyclodextrin Materials Photochemistry, Photophysics and Photobiology, Abderrazzak Douhal, 2006 Elsevier B.V.

[20] a. S.C. Szathmary, R. de Coster, Minutes International Symposium on Cyclodextrins, vol. 5, 1990, p. 518; b. S.C. Szathmary, K.U. Seiler, I. Luhmann, H.J. Huss, Minutes International Symposium on Cyclodextrins, vol. 5, 1990, p. 535; c. Y. Si, Q. Zhang, W. Jin, S. Yang, Z. Wang, D. Qu, Aqueous highly emissive host-guest systems by host enhanced intramolecular charge transfer. Dyes Pigm. 173 (2020) 107919.

[21] A.K. Tripathi, A Fluorescence Study on Binding Interaction of N-acetylated Dansylamide Conjugates with β-cyclodextrin, Tween-20 and DPPC Lipid Bilayer Membrane, J. Fluoresc. 28 (2018) 409–417.

[22] S. Zidane, A. Maiza, H. Bouleghlem, B. Fenet, Y. Chevalier, Inclusion complex of Tramadol in β-cyclodextrin enhances fluorescence by preventing self-quenching, J. Incl. Phenom. Macrocycl. Chem. 93 (2019) 253–264.

[23] H.N. Akl, A.M.M. Alazaly, D. Salah, H.S. Abdel-Samad, A.A. Abdel-Shafi, Effects on the photophysical properties of naphthylamine derivatives upon their inclusion in cyclodextrin nanocavities, J. Mol. Liq. 311 (2020) 113319.

[24] S. Dasa, S. Nathb, T.S. Singhb, N. Chattopadhyaya, Cavity size dependent stoichiometry of probe-cyclodextrin complexation: Experimental and molecular docking demonstration, J. Photochem. Photobiol. A 388 (2020) 112158.

[25] Y. Sueishi, Y. Matsumoto, J. Sohama, Y. Osawa, H. Okamoto, Distinctive effects on fluorescence quantum yields of 4-substituted *N*methylphthalimides by inclusion complexation with β-cyclodextrins, J. Incl. Phenom. Macrocycl. Chem. 93 (2019) 275–281.

[26] a. T. P. Johnston, G. S. Mc Caleb, P.S. Opliger, J. A. Montgomery, Med. Chem. 9 (1966) 892; b. T. P. Johnston, G. S. Mc Caleb, P.S. Opliger, J. A. Montgomery, J. med. Chem. 14 (1971) 600; c. J. A. Montgomery, H.J. Thomas, R. W. Brockman, G. P. Wheeler, J. Med. Chem. 24 (1981) 184.

[27] a. M. Abdaoui, G. Dewynter, N. Aouf, G. Favre, A. Morere, J.-L. Montero, Bioorg. Med. Chem. 4 (1996) 1227; b. M. Abdaoui, G. Dewynter, J.-L. Montero, Tetrahedron Lett. 37 (1996) 5695; c. M. Abdaoui, G. Dewynter, N. Aouf, J.-L. Montero, Phosphorus, Sulfur, Silicon. 118 (1996) 39; d. G. Dewynter, M. Abdaoui, Z. Regainia, J.-L. Montero, Tetrahedron. 52 (1996) 14217; e. G. Dewynter, M. Abdaoui, L. Toupet, J.-L. Montero, Tetrahedron Lett. (1997) 38, 8691; f. G. Dewynter, M. Abdaoui, L. Toupet, J.-L. Montero, Tetrahedron. 56 (2000) 2427-2435.

[28] R. Gaudraut, M.A. Alaoui-Jamali, P.X. Lacroix, Cancer Chemother. Pharmacol. 33 (1994) 489–492.

[29] J.K. Synder, L.M. Stock, Conformational preferences in alkylnitrosoureas, J. Org. Chem. 45 (5) (1980) 886–891.

[30] a. N. O. Can, D. Osmaniye, S. Levent, B. N. Sağlık, B. Korkut, O. Atlı, Y. Ozkay, Z.A. Kaplancıklı, Design, synthesis and biological assessment of new thiazolylhydrazine derivatives as selective and reversible hMAO-A inhibitors, Eur. J. Med. Chem. 144 (2018) 68-81; b. F. Cheng, W. Li, Y. Zhou, J. Shen, Z. Wu, G. Liu, P.W. Lee, Y. Tang, admetSAR: a comprehensive source and free tool for assessment of chemical ADMET properties, J. Chem. Inf. Model. 52 (2012) 3099-3105; c. C.M. Nisha, A. Kumar, A. Vimal, B.M. Bai, D. Pal, A. Kumar, Docking and ADMET prediction of few GSK-3 inhibitors divulges 6-bromoindirubin-3-oxime as a potential inhibitor. J. Mol. Graph. Journal of Molecular Graphics and Modelling. 65 (2016) 100-107; d. L.S. Goodman. The pharmacological Basis of Therapeutics, 9th edition. New York: McGraw Hill, pp. 641, 1712±1792 (1996); e. G. Klopman, L.R. Stefan, R.D. Saiakhov, ADME

evaluation: 2. A computer model for the prediction of intestinal absorption in humans. Eur. J. Pharm. Sci. 17(2002) 253- 263.
[31] C.T. Gnewuch, G. Sosnovsky, Critical appraisals of approaches for predictive designs in anticancer drugs, CMLS Cell. Mol. Life Sci. 59 (2002) 959–1023.
[32] M. Lobell, L. Molnár, G.M. Keserü, Recent advances in the prediction of blood-brain partitioning from molecular structure, J. Pharma. Sci. 92 (2) (2003) 360–370.
[33] A.K. Mishra, S.K. Dogra, Effects of Solvents and pH on the Spectral Behavior of 2-(*p*-Aminophenyl)benzimidazole, Bull. Chem. Soc. Jpn. 58 (1985) 3587–3592.
[34] T. Stalin, N. Rajendiran, Effects of solvent, pH and β-cyclodextrin on the photophysical properties of 4-hydroxy-3,5-dimethoxybenzaldehyde: intramolecular charge transfer associated with hydrogen bonding effect, Spectrochim. Acta A. 61 (2005) 3087–3096.
[35] a. M. J. Kamlet, R. W. Taft, The solvatochromic comparison method. I. The β-scale of solvent hydrogen-bond acceptor (HBA) basicities, J. Am. Chem. Soc. 98 (1976) 377-353; b. M. J. Kamlet, J. L. Abboud, R. W. Taft, The solvatochromic comparison method. 6. The π^* scale of solvent polarities, J. Am. Chem. Soc. 99 (1977) 6027-6038; c. M. J. Kamlet, J. L. M. Abboud, R. W. Taft, An examination of linear salvation energy relationships, Progr. Phys. Org. Chem. 13 (1981) 485-630; d. M. J. Kamlet, J. L. Abboud, M. H. Abraham, R. Taft, Linear salvation energy relationships. 23. A comprehensive collection of the solvatochromic parameters, π^*, α and β, and some methods for simplifying the generalized solvatochromic method, J. Org. Chem. 48 (1983) 2877-2887.
[36] a. J. Catalán, Toward a generalized treatment of the solvent effect based on four empirical scales. Dipolarity (SdP, a new scale), polarizability (SP), acidity (SA) and basicity (SB) of the medium, J. Phys. Chem. B 113 (2009) 5951-5960; b. J. C. del Valle, F. Garcia Blanco, J. Catalán, Empirical Parameters for Solvent Acidity, Basicity, Dipolarity, and Polarizability of the Ionic Liquids [BMIM][BF4] and [BMIM][PF6]. J. Phys. Chem. B 119,13 (2015) 4683-4692.
[37] C. Laurence, J. Legros, A. Chantzis, A. Phanchat, D. Jacquemin, A database of dispersion-induction DI, electrostatic ES, and hydrogen bonding α and β solventparameters and some applications to the multiparameter correlations to the multiparameter correlation analysis of solvent effects, J. Phys. Chem. B 119 (7) (2015) 3174–3184.
[38] C. Reichardt, Solvents and solvent effects in organic chemistry, 3rd edn., Wiley-VCH, Weinheim, 2003.
[39] M.J. Kamlet, R.W. Taft, Linear solvation energy relashionships. Local empirical rules – or fundamental laws of chemistry? A reply to the chemometricians, Acta Chem. Scand. B. 39 (1985) 611–628.
[40] a. N. Bensouilah, H. Fisli, N. Dhaoui, N. Benali-Cherif, M. Abdaoui, Solvent effects of N-nitroso, N-(2-chloroethyl), N′,N′-dibenzylsulfamid and its copper (II) and cobalt(II) complexes: fluorescence studies. Luminescence. 28 (2013) 30-37; b. Z. Yang, D. Shao, G. Zhou, Solubility parameter of lenalidomide for predicting the type of solubility profile and application of thermodynamic model. J. Chem. Thermodynamics. 132 (2019) 268-275; c. R. Li, L. Fu, J. Zhang, W. Wang, X. Chen, J. Zhao, D. Han, Solid-liquid equilibrium and thermodynamic properties of dipyridamole form II in pure solvents and mixture of (N-methyl pyrrolidone + isopropanol). J. Chem. Thermodynamics. 142 (2020) 105981; d. Y. Wan, H. He, R. Sun, L. Li, J. Sha, G. Jiang, Y. Li, X. Yao, T. Li, B. Ren, Solubility modeling, solvent effect and mixing properties of 5-chloro-8-hydroxyquinoline (Form I) in twelve pure solvents at various temperatures, J. Mol. Liq. 308, 15 (2020) 112988.
[41] I.B. Berlman, Evidence of intramolecular hydrogen bonding from spectroscopic data'', Chem. Phys. Lett. 3 (2) (1969) 61–63.
[42] D.M. Garrison, L.M. Doh, R.O. Potts, W. Abraham, Fluorescence spectroscopy of 9-anthroyloxy fatty acids in solvents, Chem. Phys. Lipids. 70 (2) (1994) 155–162.
[43] W. L. Hinze, F. Dai, R. P. Frankewich, K. N. Thimmaiah, J. Szejtli, Comprehensive molecular chemistry, in: J. Szejtli, T. Osa (Eds.), Cyclodextrins, vol. 3, Pergamon, Tarritown, NY. (1996) p. 587.
[44] K.A. Connors, Binding constants: the measurement of molecular complex stability, Wiley-Interscience, New York, 1987.
[45] P. Job, Formation and stability of inorganic complexes in solution, Ann. Chim. Appl. 9 (1928) 113–203.
[46] A. Beltran-Porter, D. Beltran-Porter, A. Cervilla, J.A. Ramirez, Simultaneous determination of stoichiometry, degree of condensation and stability constant A generalization of the molar-ratio method, Talanta 30 (2) (1983) 124–126.
[47] L. Liu, Q.X. Guo, The driving forces in the inclusion complexation of cyclodextrins, J. Incl. Phenom. Macrocycl. Chem. 42 (2002) 1–14.